An NMR Determination of CO Diffusion on Platinum Electrocatalysts

ARTICLE *in* JOURNAL OF THE AMERICAN CHEMICAL SOCIETY · NOVEMBER 2005

Impact Factor: 12.11 · DOI: 10.1021/ja0550475 · Source: PubMed

6 AUTHORS, INCLUDING:

Lajos Gancs
Lam Research Corporation
17 PUBLICATIONS **544** CITATIONS

J|A|C|S
COMMUNICATIONS

Published on Web 09/23/2005

An NMR Determination of CO Diffusion on Platinum Electrocatalysts

Takeshi Kobayashi, Panakkattu K. Babu, Lajos Gancs, Jong Ho Chung, Eric Oldfield,* and Andrzej Wieckowski*

Department of Chemistry, University of Illinois at Urbana−Champaign, 600 South Mathews Avenue, Urbana, Illinois 61801

Received July 26, 2005; E-mail: eo@chad.scs.uiuc.edu; andrzej@scs.uiuc.edu

Study of the diffusion of small molecules on catalyst surfaces is of broad general interest, and there have been numerous investigations of surface CO diffusion on Pt under ultrahigh vacuum (UHV) or gas phase conditions.[1−7] Both diffusion coefficients (D_{CO}) as well as activation energies (E_d) for diffusion have been measured and are of importance in the context of, among other topics, CO hydrogenation in fuel synthesis[8] and CO oxidation in heterogeneous catalysis.[9] The latter topic is also of interest in the context of fuel cell catalysis, but there has been no direct experimental determination of D_{CO} in an electrochemical environment due to problems associated with the presence of the electrolyte.[10] Fortunately, however, NMR methods are not plagued by these problems,[11−13] and in this paper, we report the first direct determination of the diffusion constants of CO on Pt in a liquid electrochemical environment, together with the activation energy for diffusion, using the techniques of electrochemical NMR (EC-NMR) [11−14] and selective spin inversion NMR.[7]

To determine diffusion constants, we used the "S-shape" pulse sequence developed by Becerra et al.[7] The S-shape pulse sequence (Figure 1) exploits the fact that CO molecules adsorbed on a Pt nanoparticle can have different ^{13}C resonance frequencies, depending on the angle of CO's unique molecular axis with respect to the external magnetic field. A part of the magnetization is selectively inverted by the first two pulses, and the ^{13}C spins are then allowed to diffuse to different regions of the nanoparticle during the evolution period T_{ev}. Motion of a CO molecule due to surface diffusion alters the ^{13}C spin's Larmor frequency (ω), and experimentally, the amplitude $M^+(T_{ev})$ of the noninverted part of the spectrum is measured for various values of T_{ev}. If only T_1 processes are involved, $M^+(T_{ev})$ grows back to its equilibrium value independent of T_{ev}, but when CO molecules diffuse, a mixing of inverted and noninverted parts of the nuclear magnetization occurs, leading to an initial decrease in $M^+(T_{ev})$, which then grows back to its equilibrium value with increasing T_{ev}.

To calculate the diffusion rate, we follow the time evolution of a normalized signal amplitude, A^+, defined by the following equation, at various T_{ev}:

$$A^+(T_{ev}) = \frac{M^+(T_{ev})\ \text{[with diffusion]}}{M^+(T_{ev})\ \text{[without diffusion]}} = \tag{1}$$

$$\frac{\sum_n A_n \sin(\lambda_n \omega_0)\exp(-\lambda_n^2 D_\omega t)\exp(-t/T_1) + \exp(-\omega_0^2/2\Delta^2)(1-\exp(-t/T_1))}{\sin(T_p\omega_0)\exp(-\omega_0^2/2\Delta^2)\exp(-t/T_1) + \exp(-\omega_0^2/2\Delta^2)(1-\exp(-t/T_1))} \tag{2}$$

where Δ is the line width and ω_0 is the frequency where $M^+(T_{ev})$ has its maximum; λ_n and A_n are the coefficients from a Fourier series solution that are determined by boundary and initial conditions.[7] D_ω (the diffusion coefficient in the frequency domain) is obtained as the sole fitting parameter to eq 2, and D_ω can then be converted to D_{CO}, the diffusion constant, using the relation, $D_{CO} = (\pi^2 d^2/32\Omega^2)D_\omega$, where d is the average particle diameter, and Ω is the upper bound for diffusion in the frequency domain, as reported elsewhere.[7]

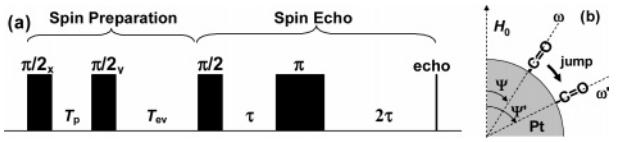

Figure 1. (a) Schematic diagram of the pulse sequence, the S-shape sequence. (b) Schematic diagram of CO surface diffusion altering the ^{13}C Larmor frequency (ω).

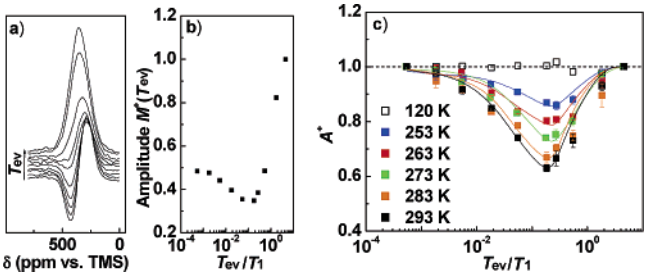

Figure 2. (a) Evolution of the ^{13}C NMR spectrum and (b) the normalized amplitude of the positive peak with T_{ev} at 293 K. (c) Experimental values of A^+ as a function of T_{ev}/T_1 for a variety of temperatures together with (solid lines) the fitted curves. Experiments were repeated at least three times at each temperature except for the 120 K data, which were recorded only once.

NMR measurements were carried out on ^{13}CO adsorbed onto electrochemically cleaned platinum black in 0.5 M D_2SO_4 using a home-built 8.47 T NMR spectrometer.[14]

Figure 2a shows the evolution of the ^{13}CO NMR spectrum as a function of T_{ev}, while the amplitude $M^+(T_{ev}/T_1)$ of the noninverted part of the spectrum at 293 K is shown in Figure 2b. $M^+(T_{ev}/T_1)$ decrease initially with increasing evolution period, then grows back to its equilibrium value, indicating that a mixing of inverted and noninverted spins occurs, due to CO diffusion.

We show in Figure 2c typical evolutions of A^+ (defined by eq 2) with T_{ev}/T_1, at six different temperatures. At 120 K, no observable CO diffusion takes place, and $A^+ = 1$ for all T_{ev}. At 253 K and above, the adsorbed CO undergoes surface diffusion and A^+ decreases due to spin mixing. In this study, we were able to fit all the measured magnetization data to a single theoretical line using eq 2, indicating a more homogeneous CO surface environment than in ref 7, where a part of the adsorbed CO was assumed to be immobile. When the temperature is increased, the activated CO diffusion results in more mixing of inverted and noninverted spins and produces a deeper trough in A^+ (Figure 2c). The D_ω values for each temperature were obtained by fitting these results to eq 2 and then converted to D_{CO}. In Figure 3a, we plot D_{CO} as a function of

10.1021/ja0550475 CCC: $30.25

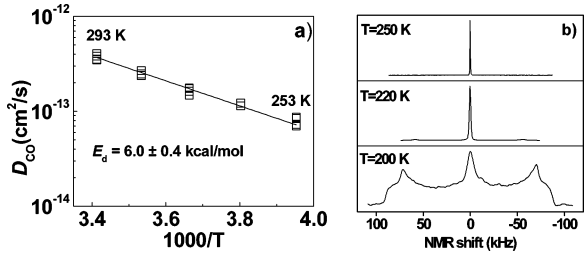

Figure 3. (a) Arrhenius plot of diffusion coefficient D_{CO}. (b) ^{2}H NMR spectra of the electrolyte as a function of temperature.

Table 1. Surface Diffusion Parameters for CO on Pt Nanoparticles

sample	θ_{CO}	E_d (kcal/mol)	D^0_{CO} (cm²/s)	D_{CO} (cm²/s)
(**In electrolyte**)				
Pt black (7 nm)	**1.00**[a]	**6.0 ± 0.4**	**1.1× 10⁻⁸**	**3.6 × 10⁻¹³**
Pt black (8 nm)[13]	∼0.5[a]	7.9 ± 2.0		
Pt/GC (3.1 nm)[19]	0.65−0.75[b]			(3 × 10⁻¹⁴)[c]
Pt/GC (1.7 nm)[16]	0.8−0.93[b]			(7 × 10⁻¹⁷)[c]
Pt/GC (1.7 nm)[17]	∼1.2[a]			(4 × 10⁻¹⁵)[d]
(**In UHV**)				
Pt/Al_2O_3 (10 nm)[7]	0.5	6.5 ± 0.5	6 × 10⁻⁷	

[a] θ_{CO} was deduced from the CO oxidation charge on cyclic voltammetry. [b] θ_{CO} was deduced from the CO oxidation at constant potential. [c] At 298 K. [d] At 294 K.

T^{-1}. The straight line (Arrhenius) fit gives an activation energy of $E_d = 6.0 \pm 0.4$ kcal/mol with a pre-exponential factor $D^0_{CO} = (1.1 \pm 0.6) \times 10^{-8}$ cm^2/s.

Figure 3b shows the ^{2}H NMR spectra of the electrolyte obtained at three different temperatures. Only below 200 K can a typical quadrupole perturbed powder pattern (expected for a spin-1 nucleus in the solid state) be seen. A weak, broad feature is visible in the spectrum recorded at 220 K, but at 250 K, the NMR spectrum is very narrow and is characteristic of an isotropic liquid.[15] This indicates that at temperatures where the CO diffusion experiments were performed (down to 253 K) the electrolyte exists in the liquid state of interest in the context of electrochemical applications.

The E_d of 6.0 kcal/mol is quite close to our previously reported estimate (7.9 ± 2.0 kcal/mol) obtained from T_2 measurements of ^{13}CO adsorbed on Pt-black[13] and also to the E_d value (6.5 ± 0.5 kcal/mol) measured for CO adsorbed on 10 nm Pt/Al_2O_3 under UHV conditions.[7] However, the value for D^0_{CO} (the pre-exponential factor) is ∼50 times smaller in the electrochemical system (Table 1), suggesting the possibility that adsorbed water and sulfate ions may impede the surface diffusion of CO.

In other work carried out in electrochemical environments,[16−18] D_{CO} was estimated from measurements of CO electrooxidation, together with model calculations. These D_{CO} values at room temperature are also shown in Table 1 and can be compared with the result obtained in this work. Our result for Pt-black (viz. 3.6 × 10^{-13} cm^2/s) is higher than the diffusion coefficient for CO for 3.1 nm Pt nanoparticles on glassy carbon (Pt/GC) that is in the 10^{-14} cm^2/s range, as recently reassessed.[19] However, on smaller particles, these values decrease significantly (4 × 10^{-15}, 7 × 10^{-17} cm^2/s).[16,17] This effect is likely due to the presence of a strong metal−support interaction in very small Pt/GC particles, resulting in an increase in the Pt Fermi level local density of states and enhanced CO bonding, as we reported previously using EC-NMR methods.[11−13] The increase in proportions of edge (corner) CO binding sites versus terrace sites may also contribute to the decrease in D_{CO} values on the smaller particles.[7,17]

In the present study, we used Pt-black saturated with adsorbed CO (∼100% CO coverage), so the surfaces of our sample have essentially no vacant Pt sites. However, a nanoparticle surface still provides a variety of sites, such as flat surfaces, edges, corners, and defects, where CO can adsorb with different binding energies. The differences between the adsorption energies of CO bound to various sites lead to a chemical potential gradient between different CO populations. We therefore propose that the surface diffusion observed here is due to CO exchange between different surface sites, a mechanism similar to that seen for diffusion of long-chain alkanes at solid/gas interfaces.[20]

These results represent the first direct NMR measurement of CO diffusion on Pt at the solid/liquid interface at and near room temperature. Between 293 and 253 K, CO diffusion follows Arrhenius behavior, with an activation energy of 6.0 ± 0.4 kcal/mol and a pre-exponential factor of (1.1 ± 0.6) × 10^{-8} cm^2/s, and at room temperature, the diffusion constant is ∼ 3.6 × 10^{-13} cm^2/s. These values should be of use in modeling the electrochemical interface, including studies of reactivity involving motions of surface CO. More generally, these results open up a new route to the study of surface diffusion of adsorbed molecules on nanoparticle electrode catalysts at the solid/liquid interface, with the possibility of correlating diffusion parameters to catalytic activity in real world applications, including the effects of catalyst modification and of applied potentials.

Acknowledgment. The authors thank Professor C. P. Slichter for useful discussions. This research was supported by grants from the U.S. National Science Foundation (CTS-02-12216) and the U.S. Department of Energy (DEFG02-91ER45439).

Supporting Information Available: Experimental details of sample preparation and NMR measurements. This material is available free of charge via the Internet at http://pubs.acs.org.

References

(1) Wang, P. K.; Ansermet, J. P.; Slichter, C. P. *Phys. Rev. Lett.* **1985**, *55*, 2731−2734.
(2) Poelsema, B.; Verheij, L. K.; Comsa, G. *Phys. Rev. Lett.* **1982**, *49*, 1731−1735.
(3) Reuttrobey, J. E.; Doren, D. J.; Chabal, Y. J.; Christman, S. B. *Phys. Rev. Lett.* **1988**, *61*, 2778−2781.
(4) Reuttrobey, J. E.; Doren, D. J.; Chabal, Y. J.; Christman, S. B. *J. Chem. Phys.* **1990**, *93*, 9113−9129.
(5) Vonoertzen, A.; Rotermund, H. H.; Nettesheim, S. *Surf. Sci.* **1994**, *311*, 322−330.
(6) Ma, J. W.; Xiao, X. D.; DiNardo, N. J.; Loy, M. M. T. *Phys. Rev. B* **1998**, *58*, 4977−4983.
(7) Becerra, L. R.; Klug, C. A.; Slichter, C. P.; Sinfelt, J. H. *J. Phys. Chem.* **1993**, *97*, 12014−12019.
(8) Xiao, X. D.; Xie, Y. L.; Jakobsen, C.; Shen, Y. R. *Phys. Rev. B* **1997**, *56*, 12529−12538.
(9) Koper, M. T. M.; Lukkien, J. J.; Jansen, A. P. J.; van Santen, R. A. *J. Phys. Chem. B* **1999**, *103*, 5522−5529.
(10) Hamnett, A.; Ertl, G.; Wieckowski, A.; Unwin, P. R.; Hillman, A. R.; Döblhofer, K.; Hayden, B. *Faraday Discuss.* **2002**, *121*.
(11) Tong, Y. Y.; Rice, C.; Wieckowski, A.; Oldfield, E. *J. Am. Chem. Soc.* **2000**, *122*, 1123−1129.
(12) Tong, Y. Y.; Kim, H. S.; Babu, P. K.; Waszczuk, P.; Wieckowski, A.; Oldfield, E. *J. Am. Chem. Soc.* **2002**, *124*, 468−473.
(13) Day, J. B.; Vuissoz, P. A.; Oldfield, E.; Wieckowski, A.; Ansermet, J. P. *J. Am. Chem. Soc.* **1996**, *118*, 13046−13050.
(14) Babu, P. K.; Kim, H. S.; Chung, J. H.; Oldfield, E.; Wieckowski, A. *J. Phys. Chem. B* **2004**, *108*, 20228−20232.
(15) Witterbort, R. J.; Usha, M. G.; Ruben, D. J.; Wemmer, D. E.; Pines, A. *J. Am. Chem. Soc.* **1988**, *110*, 5668−5671.
(16) Maillard, F.; Eikerling, M.; Cherstiouk, O. V.; Schreier, S.; Savinova, E.; Stimming, U. *Faraday Discuss.* **2004**, *125*, 357−377.
(17) Cherstiouk, O. V.; Simonov, P. A.; Zaikovskii, V. I.; Savinova, E. R. *J. Electroanal. Chem.* **2003**, *554*, 241−251.
(18) Lebedeva, N. P.; Rodes, A.; Feliu, J. M.; Koper, M. T. M.; van Santen, R. A. *J. Phys. Chem. B* **2002**, *106*, 9863−9872.
(19) F. Maillard, private communication.
(20) Lazar, P.; Schollmeyer, H.; Riegler, H. *Phys. Rev. Lett.* **2005**, *94*, 116101.

JA0550475